RSC Advances

PAPER

View Article Online
View Journal | View Issue

Cite this: *RSC Adv.*, 2016, **6**, 103650

PdGa/TiO_2 an efficient heterogeneous catalyst for direct methylation of *N*-methylaniline with CO_2/H_2†

Xinluona Su,[abc] Weiwei Lin,*[bc] Haiyang Cheng,[bc] Chao Zhang,[bc] Yan Li,[bc] Tong Liu,[bcd] Bin Zhang,[bcd] Qifan Wu,[bcd] Xiujuan Yu*[a] and Fengyu Zhao*[bc]

Received 3rd September 2016
Accepted 17th October 2016

DOI: 10.1039/c6ra22089d

www.rsc.org/advances

An effective sustainable heterogeneous PdGa/TiO_2 catalyst was prepared for direct methylation of *N*-methylaniline with CO_2/H_2 to *N*,*N*-dimethylaniline. The PdGa/TiO_2 catalyst exhibited 98% conversion and 94% selectivity under the reaction conditions (180 °C, 5 MPa H_2, 5 MPa CO_2, 10 h), which are one of the best results reported to date for the heterogeneous *N*-methylation with CO_2 as methylation reagent over the supported metal catalysts. The PdGa/TiO_2 catalyst was well characterized using TEM, TPR, XPS, CO-adsorption IR studies and high-pressure *in situ* FTIR studies. It was confirmed that PdGa bimetallic alloy nanoparticles were formed and highly dispersed on the TiO_2 support, and the electron-deficient Pd derived from the interaction with Ga could activate CO_2 and transform it to formic acid, which is the key step for the discussed methylation, and high activity was obtained over the PdGa/TiO_2 catalyst. The activating properties of the PdGa/TiO_2 catalyst will open a new route for transfer and utilization of CO_2 in the fields of energy and environmental fields.

Introduction

The *N*-methylation of amines is an important reaction in the organic synthesis and chemical industry, as it can produce pharmaceuticals, agrochemicals, dyes, perfumes, and key intermediates.[1,2] Therefore, the development of an efficient and green methylation process has attracted much attention. Recently, CO_2 as a green and renewable carbon resource was used for the *N*-methylation reaction to replace the conventional methylation reagent, such as methyl iodide and diazomethane.[3–7] However, the application of CO_2 as a raw material in chemical synthesis is extremely difficult because of its thermodynamic stability. Therefore, exploring a suitable active catalyst to activate CO_2 is an important key issue in the utilization and transfer of CO_2 to value-added chemicals and fuel or energy compounds. In 2013, Cantat *et al.*[5] reported for the first time that *N*-methylation reaction can be performed using CO_2 as methyl reagent in the presence of zinc salts catalyst and hydrosilanes reductant. Leitner *et al.*[8] and Beller *et al.*[9] independently reported the methylation of amines with CO_2 in the presence of homogeneous Ru complex catalysts and hydrosilane. Subsequently, Dyson *et al.*[10] reported a metal-free homogeneous catalyst for the methylation of amines with CO_2 and a hydrosilane reductant. Shortly afterwards, a greener and effective method for the methylation of amines with homogeneous Ru-based catalysts was reported by Beller *et al.*;[11] they used CO_2 as a methyl reagent and H_2 as reducing agent to replace hydrosilanes, in which water was generated as a sole by-product. Moreover, a heterogeneous catalyst for the *N*-methylation reaction with CO_2 and H_2 was studied. This can settle the problems of homogeneous catalysts, such as the inability to reuse, difficult catalyst/product separation, and the necessity of additives (ligands, acids, and salts). It was reported that $CuAlO_x$ and $PdCuZrO_x$ were effective for the methylation of amines with CO_2 and H_2, and a high product yield of about 96% was achieved.[12,13] In addition, Shimizu *et al.*[14] reported a metal supported heterogeneous catalyst of Pt-MoO_x/TiO_2 to be effective for *N*-methylation with CO_2 and H_2, in which they discussed the possible intermediates and proposed a plausible reaction mechanism that formic acid was first formed by the Pt-catalyzed hydrogenation of CO_2, then reacts with amine to give *N*-methylformanilide, and finally undergoes Pt-catalyzed hydrogenation to give a tertiary amine. This is the first report of the reaction mechanism of *N*-methylation with CO_2 and H_2; it provides important information and reference for a further study of this *N*-methylation reaction system. Inspired by this result, we then focussed on the preparation of an efficient catalyst that can activate CO_2 and transfer it to formic acid as

[a]*Department of Environmental Science and Engineering, Heilongjiang University, Harbin, 150080, P. R. China. E-mail: yuxiujuan@hlju.edu.cn*

[b]*State Key Laboratory of Electroanalytical Chemistry, Changchun Institute of Applied Chemistry, Chinese Academy of Sciences (CAS), Changchun 130022, P. R. China. E-mail: fyzhao@ciac.ac.cn; linwei@ciac.ac.cn*

[c]*Laboratory of Green Chemistry and Process, Changchun Institute of Applied Chemistry, CAS, Changchun 130022, P. R. China*

[d]*University of Chinese Academy of Sciences, Beijing 100049, P. R. China*

† Electronic supplementary information (ESI) available. See DOI: 10.1039/c6ra22089d

well as aid in hydrogenation of *N*-methylformanilide, an intermediate of methylation. We prepared a $PdGa/TiO_2$ catalyst for the *N*-methylation reaction of *N*-methylaniline with CO_2 and H_2 because PdGa was reported to be active for the hydrogenation of CO_2, and Ga_2O_3 could promote the activity of Pd/SiO_2 in the production of methanol from CO_2 reduction.[15,16] The $PdGa/TiO_2$ catalyst presented higher activity compared to Pd/TiO_2. The reaction mechanism was discussed in detail using the CO-adsorption IR and high-pressure *in situ* FTIR spectra combining with the results of the control experiments. It was confirmed that the PdGa bimetallic alloy nanoparticles were formed and highly dispersed on the TiO_2 support, and the electron-deficient Pd derived from the interaction with Ga could activate CO_2 and transform it to formic acid, which is the key step for the discussed methylation; high activity was obtained over the $PdGa/TiO_2$ catalyst compared to Pd/TiO_2.

Experimental

Catalyst preparation

All chemicals used in this experiment were of analytical grade and used without further purification. TiO_2(P25) was used as the support, and $PdCl_2$ and $Ga(NO_3)_3$ were used as the metal precursors. Pd/TiO_2 was prepared by deposition–precipitation (DP) using Na_2CO_3 as the precipitating agent. In a typical procedure, the support TiO_2 was added to an aqueous solution containing $PdCl_2$, and the suspension was placed into a water bath maintained at 35 °C. The Na_2CO_3 solution (1 mol l^{-1}) was then added dropwise into the suspension until the pH was adjusted to 10.0 with vigorous stirring. After the DP procedure, the precipitate was collected, washed with water, and then vacuum-dried, and finally calcined under a flow of air at 350 °C for 4 h.

The Ga-modified Pd/TiO_2 catalysts were prepared by a co-precipitation method. The TiO_2 support was added to an aqueous solution containing a given amount of $PdCl_2$ and $Ga(NO_3)_3$ and the further procedure was the same as that of Pd/TiO_2. The Ga content was varied with a Ga/Pd mole ratio of 1/1, 3/1 and 6/1. The as-prepared catalysts were labeled as $PdGa/TiO_2$(1), $PdGa/TiO_2$(3), $PdGa/TiO_2$(6) (1, 3 and 6 in parenthesis refers to the mole ratio of Ga/Pd). The Pd content in all the catalysts was about 3 wt% as examined by inductively coupled plasma-optical emission spectrometry (ICP).

Catalyst characterization

Powder XRD was performed using a Bruker D8 Advance X-ray diffractometer with a Cu Kα source at 40 kV and 40 mA, at 2θ from 10° to 90° with 4° min^{-1} speed.

TEM was carried out in a JEOL JEM-2010 instrument at an accelerating voltage of 200 kV. High-angle annular dark-field scanning transmission electron microscopy (HAADF-STEM) images and element analysis mapping were collected on a Tecnai G2 F30 transmission electron microscope operating at 200 kV (FEI company). The STEM, elemental analysis mapping and EDS line scanning were determined by Titan 80-300 Cs-corrected TEM with a resolution 0.08 nm at 300 kV.

Hydrogen temperature-programmed reduction (H_2-TPR) experiments were performed using a Micromeritics AutoChem II 2920 Automated Catalyst Characterization System. Prior to the experiment, 50 mg sample was loaded into a U-shaped quartz reactor and pretreated with Ar at 150 °C for 30 min to remove the adsorbed water. After cooling to 50 °C, 10 vol% H_2/Ar mixed gas was passed into the sample, and then heated to 800 °C at a ramping rate of 10 °C min^{-1}. Hydrogen consumption was determined using a thermal conduction detector (TCD).

X-ray photoelectron spectroscopy (XPS, VG Microtech 3000 Multilab) was used to measure the electronic properties of Pd and Ga on the surface of the Pd/TiO_2 and $PdGa/TiO_2$ catalysts. The C 1s peak at 284.6 eV arising from the adventitious carbon was used as a reference. This reference gives binding energy values with a precision of ±0.02 eV. The surface composition of the samples was determined from the peak areas of the corresponding lines using a Shirley type background and empirical cross-section factors for XPS.

In situ diffuse reflectance infrared Fourier-transformed (DRIFT) spectra of CO adsorption were collected using a Nicolet iS50 spectrometer equipped with a MCT detector. Before the experiment, all the catalysts were reduced *in situ* with 10% H_2–Ar (70 ml min^{-1}) at 200 °C for 0.5 h. The flowing gas was switched to He (70 ml min^{-1}) at the same temperature to remove the residual H_2 and Ar. After that, the sample was cooled to 30 °C and a background spectrum was collected. This was automatically subtracted from the measured spectra. Subsequently, the sample was exposed to 10% CO–He at a flow rate of 70 ml min^{-1} for about 30 min. Finally, the sample was purged by He for another 15 min and the spectra were recorded. In all cases, the spectra were taken at 30 °C, with a resolution of 4 cm^{-1} and cumulative 32 scans.

In situ high-pressure FTIR spectra were performed in a high-pressure reaction cell with ZnSe windows using a Nicolet iS50 spectrometer equipped with a MCT detector. After loading the sample, the cell was purged with H_2 a few times to remove the air and heated to 200 °C. H_2 was further introduced until the pressure reached 2 MPa and maintained at this temperature for 30 min. The cell was cooled to 30 °C, purged again with atmospheric H_2 a few times, introduced with 2 MPa H_2 and 4 MPa CO_2 and a background spectrum was collected. The cell was then heated to 180 °C and maintained at this temperature for 30 min. After that, the cell was cooled to 30 °C and the spectra were collected. The gases in the cell were released to ambient pressure and the tested sample was purged by He for 5 min and FTIR spectra were further collected.

Activity test

The *N*-methylation of *N*-methylaniline with CO_2/H_2 was carried out in a 50 ml stainless steel autoclave reactor at 180 °C. Prior to the reaction, all the catalysts were reduced in a quartz tube at 400 °C with a flow of hydrogen (30 ml min^{-1}) for 2 h. Certain amounts of *N*-methylaniline (1 mmol), solvent (*n*-octane 2 ml) and catalysts (metal 0.3 mol%) were added into the reactor, and the reactor was sealed and flushed with 1 MPa H_2 at least three

times to remove the air. The reactor was then heated to 180 °C in an oil bath and introduced with 5 MPa H_2 first and then 5 MPa CO_2 with a high-pressure liquid pump. The reaction was started with continuous stirring. When the reaction was finished, the reactor was cooled to room temperature in an ice-water bath and mix gas was then vented at ambient pressure. The liquid products were analyzed with a gas chromatograph (Shimadzu GC-2010, Rtx-5 capillary column) using a flame ionization detector and identified by gas chromatography/mass spectrometry (GC/MS, Agilent 5890). The GC results were obtained using an internal standard method and biphenyl as a standard substrate. The conversion and selectivity were calculated using the following equations.

$$\text{MA conversion } (\%) = \left(1 - \frac{\text{remaining amount of MA}}{\text{Initial amount of MA}}\right) \times 100\% \quad (1)$$

$$\text{DMA selectivity } (\%) = \frac{\text{Amount of DMA produced}}{\text{Sum of the amounts of all the products}} \times 100\% \quad (2)$$

Results and discussion

Characterization of Pd/TiO_2 and $PdGa/TiO_2$ catalysts

TiO_2-supported Pd catalyst (Pd/TiO_2) and Ga-modified Pd catalysts ($PdGa/TiO_2$) were prepared by deposition–precipitation, and the powder XRD patterns of precursors are shown in Fig. 1. All the samples displayed the characteristic diffraction peaks of the typical TiO_2, but no diffraction peaks were found for Pd and Ga or their metallic compounds, which should be ascribed to the low metal loadings or the fine dispersion of the Pd and Ga species on the surface of TiO_2.

The dispersion of Pd or PdGa particles on the TiO_2 was characterized by TEM and element analysis mapping with line scanning. As shown in Fig. 2, both Pd and PdGa nanoparticles were well dispersed on the support of TiO_2 and Pd/TiO_2 and $PdGa/TiO_2$ catalysts had a similar distribution with an average metal particle size of around 3 nm, indicating that the addition of Ga did not affect the Pd distribution. STEM images and EDX

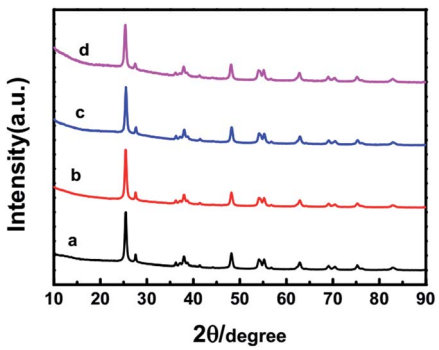

Fig. 1 XRD patterns of (a) Pd/TiO_2, (b) $PdGa/TiO_2(1)$, (c) $PdGa/TiO_2(3)$, and (d) $PdGa/TiO_2(6)$.

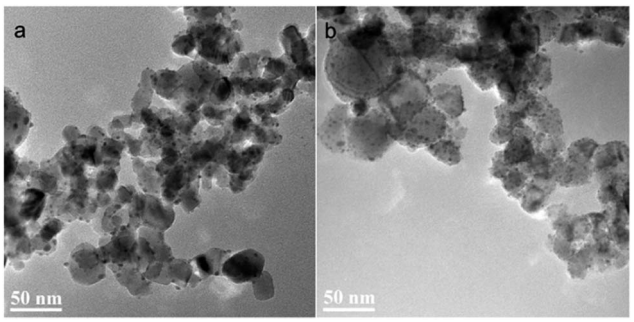

Fig. 2 TEM images of catalysts (a) Pd/TiO_2, (b) $PdGa/TiO_2(6)$ catalysts.

elements mapping for the $PdGa/TiO_2(6)$ catalyst in Fig. 3b and c indicated that Pd and Ga show similar distribution on the surface of TiO_2, indicating that Ga deposits with Pd together. This was further confirmed by STEM and the EDX line profile of the Pd-L and Ga-L signals across a single particle, as shown in Fig. 4. It is clear that there is no segregation of Pd and Ga and they are very well coherent together, which suggests the formation of PdGa bimetallic compounds or PdGa nanoalloys on the surface of TiO_2. This was further demonstrated by XPS and CO-FTIR.

The TPR experiments were performed to determine the redox properties of the catalysts. For the Pd/TiO_2 catalyst (Fig. 5a), a negative peak centred at about 70 °C corresponds to β-PdH_x decomposition and a peak at around 220 °C is ascribed to the reduction of Pd^{2+} having a strong interaction with TiO_2 support, and the peak at around 512 °C is ascribed to the reduction of TiO_2 ($Ti^{4+} \rightarrow Ti^{3+}$); this process is promoted by the presence of

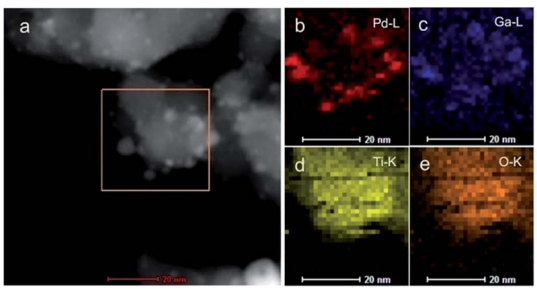

Fig. 3 STEM (a) for $PdGa/TiO_2(6)$ catalyst and its corresponding elemental mapping images of (b) Pd-L, (c) Ga-L, (d) Ti-K, (e) O-K.

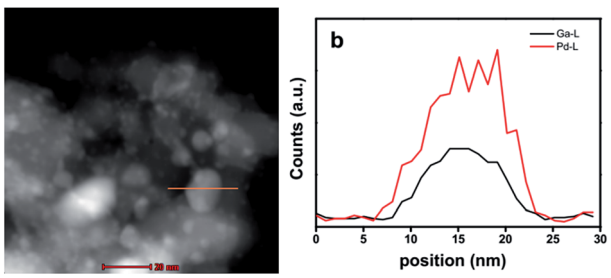

Fig. 4 (a) STEM-HAADF image of the $PdGa/TiO_2(6)$ catalyst; (b) X-EDS line scanning spectra of the selected metal particles.

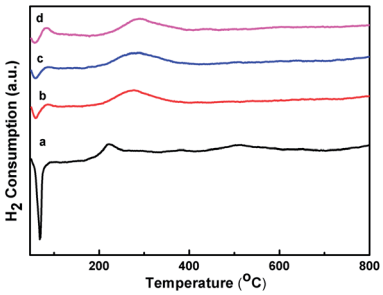

Fig. 5 H_2-TPR profiles of (a) Pd/TiO_2, (b) $PdGa/TiO_2(1)$, (c) $PdGa/TiO_2(3)$, and (d) $PdGa/TiO_2(6)$.

dispersed metal crystallites.[17] As for the $PdGa/TiO_2$ catalysts (Fig. 5b–d), a similar negative peak centred at about 70 °C for the β-PdH_x decomposition was also observed, but it was much smaller than that of the Pd/TiO_2 catalyst (Fig. 5a), suggesting that the presence of Ga has an influence on the reduction behaviour. The peak at around 83 °C and its intensity or area increased with increasing Ga content, which was assigned to the reduction of the Pd species neighboured to Ga. Moreover, a peak presented at around 288 °C moved slightly to the higher temperature on increasing the Ga content, which was attributed to the reduction of Ga species adjacent to Pd, suggesting that the interaction between Pd species and Ga species was stronger and the presence of Pd could accelerate the reduction of gallium oxide moieties.[18] It was reported that pure Ga_2O_3 would not undergo reduction in hydrogen until 900 °C.[19] The peak at around 512 °C for the reduction of TiO_2 was not found in the $PdGa/TiO_2$ catalysts, it is assumed that the presence of Ga reduced the interaction of Pd and TiO_2.

To further certify the interactions among Pd, Ga and TiO_2, the surface properties and the electronic states of Pd and Ga were analyzed by XPS, and the results are shown in Fig. 6. For Pd/TiO_2 catalyst, the Pd 3d spectra showed two main peaks at the binding energy around 334.4 eV and 339.8 eV, which are in accordance with the literature values for Pd $3d_{5/2}$ and Pd $3d_{3/2}$ of Pd^0, indicating that Pd exists mainly as a metallic phase in the Pd/TiO_2 catalyst.[20] As for $PdGa/TiO_2(1)$ catalyst, the binding energy shifted to 334.6 eV, 0.2 eV higher compared to that of Pd/TiO_2; the binding energy further increased with increasing content of Ga, about 0.3 eV and 0.4 eV shift for $PdGa/TiO_2(3)$ and $PdGa/TiO_2(6)$, respectively. This suggested that the presence of Ga leads Pd to be more positive because of the electron transfer from Pd to Ga species. The above results clearly revealed the strong interaction between Pd and Ga, and the electronic environment of Pd was modified with the addition of Ga, which corresponds to a shift of the binding energy of the Ga 3d spectra. For the Ga_2O_3/TiO_2 catalysts, Ga 3d showed two peaks at 20.0 eV and 21.6 eV, ascribing to Ga^+ and Ga^{3+}, respectively.[21,22] This suggests that Ga is barely reduced at 400 °C. For the $PdGa/TiO_2$ catalysts, Ga 3d showed three peaks at 18.9 eV, 19.9 eV and 21.5 eV, ascribing to Ga^0, Ga^+ and Ga^{3+}, respectively.[23,24] This indicates that a part of Ga^{3+} was partially reduced to Ga^0 during the reduction in the presence of Pd. Moreover, it is evident that with increasing Ga content, the Ga^0 peaks shift to lower binding energies (18.5 eV to 21.4 eV), which indicates a strong electron interaction between Pd and Ga species for the formation of the PdGa bimetallic compounds, in which Pd is electron deficient and Ga electron enriched. This finding is in accordance with literature, where Haghofer *et al.* reported that a Pd_2Ga bimetallic alloy could form on the surface of Pd/Ga_2O_3,[25] and Collins *et al.* reported a series of Pd_5Ga_2, Pd_5Ga_3, and Pd_2Ga bimetallic alloy compounds formed under the reduction temperature above 300 °C on the surface of Pd/Ga_2O_3.[26] In the present study, the XRD pattern for the $PdGa/TiO_2$ catalysts was also measured, shown in Fig. 1, but we did not find the diffraction patterns of Pd or PdGa, except for the diffraction of TiO_2, due to their low loading.

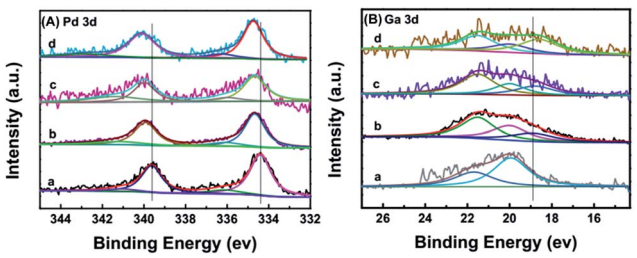

Fig. 6 (A) Pd 3d XPS spectra of catalysts (a) Pd/TiO_2, (b) $PdGa/TiO_2(1)$, (c) $PdGa/TiO_2(3)$, and (d) $PdGa/TiO_2(6)$; (B) Ga 3d XPS spectra of catalysts (a) Ga/TiO_2, (b) Pd/TiO_2, (c) $PdGa/TiO_2(1)$ and (d) $PdGa/TiO_2(3)$.

Catalytic performances of Pd/TiO_2 and $PdGa/TiO_2$

The catalytic performance of Pd/TiO_2 and $PdGa/TiO_2$ catalysts was checked and compared for the methylation of *N*-methyl-aniline (MA) to *N*,*N*-dimethyl aniline (DMA) with CO_2 and H_2. As shown in Table 1, the conversion of MA was 34.7% and the selectivity of DMA was 8% over the Pd/TiO_2 catalyst. In comparison, the addition of a small amount Ga species to the Pd/TiO_2 catalyst could improve the conversion of MA and the selectivity of DMA prominently, and with increasing of Ga content, the conversion increased and reached a maximum value of 92.9% over the $PdGa/TiO_2(6)$ (with a Ga : Pd mole ratio of 6). On the other hand, the conversion then decreased to

Table 1 Results for the methylation of *N*-methyl aniline over different catalysts[a]

Entry	Catalyst	Conv. (%)	Sel.[b] (%) DMA	MFA	AN	FA
1	Pd/TiO_2	34.7	8.0	4.6	9.3	78.1
2	$PdGa/TiO_2(1)$	46.9	72.0	3.4	23.7	0.8
3	$PdGa/TiO_2(3)$	64.3	83.1	2.5	14.4	—
4	$PdGa/TiO_2(6)$	92.9	90.3	4.2	9.3	—
5	$PdGa/TiO_2(10)$	88.2	95.0	0.4	4.65	—
6	Ga_2O_3/TiO_2	13.1	31.9	59.3	8.2	0.6

[a] Reaction conditions: MA 1 mmol, CO_2 5 MPa, H_2 5 MPa, octane 2 ml, catalyst 0.3 mol% Pd to MA, 180 °C, 8 h. [b] *N*,*N*-Dimethylaniline (DMA), *N*-methylformanilide (MFA), aniline (AN), *N*-phenylformamide (FA).

88.2% with further increase in Ga content over the PdGa/TiO_2(10), and the Ga_2O_3/TiO_2 catalyst gave poor activity (entry 7). It is evident that the addition of Ga species could improve the catalytic performance of Pd largely by electron modification *via* the formation of PdGa bimetallic alloy compounds on the surface of TiO_2.

Fig. 7 shows the change in the conversion and products selectivity with reaction time over PdGa/TiO_2(6) catalyst. The conversion of MA was 40% at a reaction running for 2 h and reached 98% at a reaction time of 10 h. With prolonging reaction time, the selectivity of DMA increased from 78% to 94%, and the selectivity of MFA decreased slightly, indicating that MFA is an intermediate and it could be transferred to the final product of DMA. The activity of the PdGa/TiO_2 catalyst was compared with several catalysts including homogeneous and heterogeneous ones, as reported recently for the direct methylation of *N*-methylaniline with CO_2/H_2 (Table S1†). PdGa/TiO_2 can be considered as the best catalyst as it gave the highest yield of the desired product of DMA. In addition, the efficiency of the PdGa/TiO_2 catalyst was checked for several amines with different structures (Table S2†). This shows that PdGa/TiO_2 was active for all the selected substrates, but the reactivity and efficiency depends on the molecular structure of the amines. The cyclic amines gave a higher yield compared to the aliphatic amines, which showed less reactivity under similar reaction conditions.

For the methylation of *N*-methylaniline with CO_2/H_2, in the catalysis mechanism of PdGa/TiO_2, both the intermediate and rate-controlling step are important. To reveal the catalytic mechanism and reaction pathway, we collected the results of several control experiments and combined them with *in situ* CO-IR spectroscopy analysis of Pd/TiO_2 and PdGa/TiO_2 catalysts. It was reported that the *N*-methylaniline was carbonylated with CO_2/H_2 first to generate an *N*-methylformanilide intermediate and it was then quickly hydrogenated to *N*-methylaniline.[13,27] The catalytic activity of Pd/TiO_2 and PdGa/TiO_2 in the two abovementioned possible reaction steps of the formation of the intermediate of *N*-methylformanilide and the hydrogenation reaction were checked and discussed. As observed from the results in Table 2, the hydrogenation of *N*-methylformanilide was a faster step, it could reach a 99.6% conversion and 77.6% selectivity within 2 h over the PdGa/TiO_2(6) catalyst. In contrast, the Pd/TiO_2 was less active irrespective of the presence or absence of CO_2, and the *N*-methylformanilide could transfer to *N*-methylaniline by a broken C–N bond, however it be reduced over the PdGa/TiO_2 catalyst under the *N*-methylation reaction conditions.

The *N*-methylation of methylaniline was then carried out using methanol, formic acid or CO as the methyl source because they are generally produced from CO_2 hydrogenation.[6,28] As observed from the results shown in Table 3, formic acid is effective, and a higher conversion was obtained with both the Pd/TiO_2 and PdGa/TiO_2 catalysts, whereas CO and methanol were found to be less active. Moreover, the conversion was much higher over the Pd/TiO_2 catalyst in the presence of formic acid, indicating that the formation of formic acid is the key step in the methylation reaction with CO_2/H_2. PdGa/TiO_2 was assumed to be more active and efficient for the production of formic acid compared to Pd/TiO_2 catalyst, which was discussed and confirmed using the *in situ* high-pressure FTIR spectra under the reaction conditions, as shown in Fig. 8. For Pd/TiO_2 catalyst (Fig. 8A(a)), the band at 1614 cm^{-1} was assigned to carbonate type species and physisorbed water on the support.[29,30] For both PdGa/TiO_2(1) and PdGa/TiO_2(6) catalysts, the bands at 1284 cm^{-1} and 1624 cm^{-1} were assigned to carbonate type species, the bands at around 1360 cm^{-1}, 1387 cm^{-1} and 1579 cm^{-1} were formate species,[10,21] and the band at 1978 cm^{-1} was the CO species.[28] After H_2 and CO_2 were released and then purged He for 5 min, H_2 and CO_2 were released, and

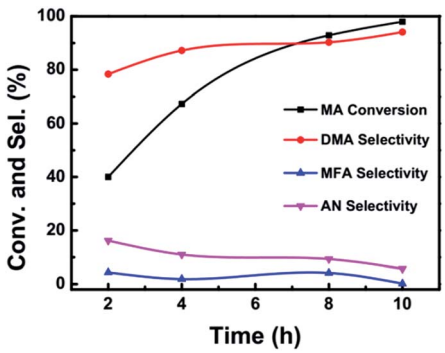

Fig. 7 Variation of conversion and selectivity with the reaction time in the methylation of *N*-methylaniline to *N*,*N*-dimethyl aniline over PdGa/TiO_2(6) catalyst.

Table 2 Catalytic performance for *N*-methylformanilide hydrogenation over different catalysts[a]

Entry	Catalyst	Conv. (%)	Sel. (%) MA	DMA	AN	FA
1	PdGa/TiO_2(1)	98	38.1	55.5	6	0.5
2	PdGa/TiO_2(6)	99.6	13.4	77.4	9.1	—
3	Pd/TiO_2	33.9	69.3	16.0	3.9	11
4	PdGa/TiO_2(6)	100	34.2	54.3	11.2	0.3
5	Pd/TiO_2[b]	56.4	63	3.9	2.4	30.7

[a] Reaction conditions: MFA 1 mmol, CO_2 5 MPa, H_2 5 MPa, octane 2 ml, catalyst 0.3 mol% Pd to MA, 180 °C, 2 h. [b] Without CO_2.

Table 3 Results for *N*-methylaniline methylation with different carbon resources[a]

Catalyst	Carbon resource	Conv. (%)	Sel. (%) DMA	MFA	AN	FA
PdGa/TiO_2	Formic acid	60	93	0.3	6.8	—
	Methanol	8.8	24	—	70.7	5.3
	CO/0.6 MPa	12.7	76.6	0.2	22.1	—
Pd/TiO_2	Formic acid	98.2	0.9	95.3	0.5	3.8
	CO/0.6 MPa	13.5	10	69.4	8.6	11.7

[a] Reaction conditions: MA 1 mmol, catalyst 0.3 mol% Pd to MA, H_2 5 MPa, octane 2 ml, 180 °C, 8 h.

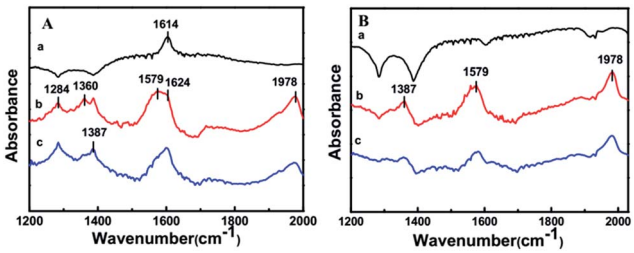

Fig. 8 High-pressure FTIR absorption spectra of CO_2 and H_2 adsorption on A: (a) Pd/TiO_2, (b) $PdGa/TiO_2(1)$ and (c) $PdGa/TiO_2(6)$ (CO_2: 4 MPa and H_2: 2 MPa). B: (a) Pd/TiO_2, (b) $PdGa/TiO_2(1)$ and (c) $PdGa/TiO_2(6)$ (after gas escape).

therefore the absorption band at 1614 cm^{-1} resulting from the surface of Pd/TiO_2 catalyst disappeared (Fig. 8B(a)). For the $PdGa/TiO_2$ catalysts, however, the absorption bands at about 1284 cm^{-1} and 1624 cm^{-1} disappeared, whereas the bands at 1387 cm^{-1}, 1579 cm^{-1} and 1978 cm^{-1} remained (Fig. 8B(b and c)). These results indicate the formation of the formate and CO species on the surface of $PdGa/TiO_2$ catalysts, resulting upon exposure to H_2 and CO_2 at 180 °C, which are much lower in concentration and weaker on the Pd/TiO_2 catalyst.

To examine the surface adsorption properties of Pd/TiO_2 and $PdGa/TiO_2$ catalysts, *in situ* CO-IR spectroscopy was performed. It is well known that peaks corresponding to the CO adsorption on Pd-based catalysts generally appeared in two main regions: the first one at 2100–2030 cm^{-1}, named as linearly adsorbed CO band, and the other around 2000–1800 cm^{-1} range, which was attributed to the bridged adsorbed CO species.[30–33] The *in situ* DRIFT spectra of CO adsorption for the catalysts with different Ga contents are shown in Fig. 9. For the Pd/TiO_2 catalyst, the vibration bands of the linear and bridge-bonded CO were presented at about 2090 cm^{-1} and 1988 cm^{-1}, respectively. For the $PdGa/TiO_2(6)$ catalyst, these bands appeared at 2085 cm^{-1} and 1978 cm^{-1}, respectively. Evidently, it has a significant red shift with about 10 cm^{-1} for the $PdGa/TiO_2(6)$ compared to Pd/TiO_2. Generally, the red-shift can be explained by geometric and electronic effects.[25,34] In the present study, the neighboring Ga atoms increased the electronic density of Pd and changed its adsorption properties. It is also found that the ratio of linear to bridge adsorption increased with increasing Ga content. Both

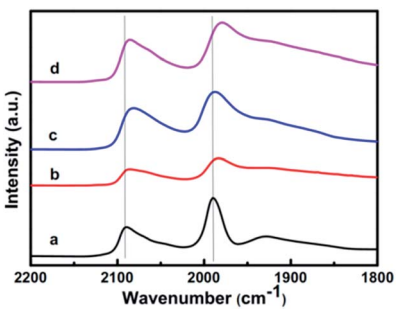

Fig. 9 *In situ* Fourier-transformed infrared spectra of CO adsorption on (a) Pd/TiO_2, (b) $PdGa/TiO_2(1)$, (c) $PdGa/TiO_2(3)$, and (d) $PdGa/TiO_2(6)$.

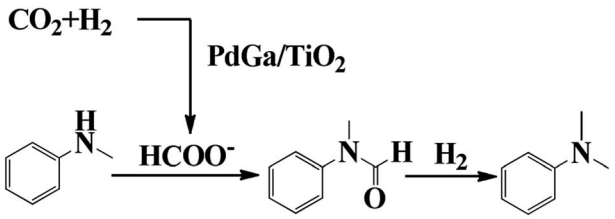

Scheme 1 Reaction pathway of Pd-catalyzed methylation of *N*-methylaniline with CO_2 and H_2.

the red-shift and the changes in adsorption intensity of CO indicated the electronic interaction between Pd and Ga as the PdGa nanoalloy formed on the TiO_2 support. Thus, the CO_2 was activated by the PdGa nanoparticles on the surface of the $PdGa/TiO_2$ catalyst and formed formic acid.

Based on the abovementioned analysis, it is confirmed that the methylation of *N*-methylaniline with CO_2/H_2 over the $PdGa/TiO_2$ catalyst should consist of the following three steps, as shown in Scheme 1: (1) formic acid formation from the reaction of CO_2 with H_2 on the surface of the $PdGa/TiO_2$ catalyst; (2) *N*-methylation reaction of *N*-methylaniline with the *in situ* formed formic acid to produce the intermediate, *N*-methylformanilide; (3) hydrogenation of *N*-methylformanilide to the final product of *N*,*N*-dimethyl aniline.

Conclusion

High efficient heterogeneous catalyst of $PdGa/TiO_2$ was developed for the direct *N*-methylation of *N*-methylaniline with CO_2/H_2. Compared to the Pd/TiO_2 catalyst, much higher conversion and selectivity to DMA were obtained with $PdGa/TiO_2$ catalysts. The strong interaction between Pd and Ga was demonstrated as PdGa bimetallic alloy particles were formed on the surface of the $PdGa/TiO_2$ catalyst, and the electron-deficient Pd could activate CO_2 and transfer it with H_2 to formic acid, which is the key step for the discussed methylation. The excellent catalytic performance of the $PdGa/TiO_2$ catalyst and its special properties in activating CO_2 will attract considerable attention of researchers in the fields of green and environmental chemistry; its potential catalytic properties and wide applications are expected.

Acknowledgements

The authors gratefully acknowledge the financial support from the NSFC (21273222, 21603212, 21311140166), and the MOST (2016YFA0602901) of China.

Notes and references

1 Z. Rappoport, *The Chemistry of Anilines*, Wiley InterScience, 2007.
2 K. Weissermel and H. J. Arpe, *Industrial Organic Chemistry*, Wiley-VCH, Weinheim, 2003.

3 A. Tlili, X. Frogneux, E. Blondiaux and T. Cantat, *Angew. Chem., Int. Ed.*, 2014, **53**, 2543–2545.
4 G. Tang, H.-L. Bao, C. Jin, X.-H. Zhong and X.-L. Du, *RSC Adv.*, 2015, **5**, 99678–99687.
5 A. Tlili, E. Blondiaux, X. Frogneux and T. Cantat, *Green Chem.*, 2015, **17**, 157–168.
6 A. Bansode, B. Tidona, P. R. von Rohr and A. Urakawa, *Catal. Sci. Technol.*, 2013, **3**, 767–778.
7 O. Jacquet, X. Frogneux, C. D. Gomes and T. Cantat, *Chem. Sci.*, 2013, **4**, 2127–2131.
8 K. Beydoun, G. Ghattas, K. Thenert, J. Klankermayer and W. Leitner, *Angew. Chem., Int. Ed.*, 2014, **53**, 11010–11014.
9 Y. Li, X. Fang, K. Junge and M. Beller, *Angew. Chem., Int. Ed.*, 2013, **52**, 9568–9571.
10 S. Das, F. D. Bobbink, G. Laurenczy and P. J. Dyson, *Angew. Chem., Int. Ed.*, 2014, **53**, 12876–12879.
11 Y. Li, I. Sorribes, T. Yan, K. Junge and M. Beller, *Angew. Chem., Int. Ed.*, 2013, **52**, 12156–12160.
12 X. Cui, X. Dai, Y. Zhang, Y. Deng and F. Shi, *Chem. Sci.*, 2014, **5**, 649–655.
13 X. Cui, Y. Zhang, Y. Deng and F. Shi, *Chem. Commun.*, 2014, **50**, 13521–13524.
14 K. Kon, S. Siddiki, W. Onodera and K. Shimizu, *Chem.–Eur. J.*, 2014, **20**, 6264–6267.
15 S. E. Collins, D. L. Chiavassa, A. L. Bonivardi and M. A. Baltanás, *Catal. Lett.*, 2005, **103**, 83–88.
16 T. Fujitani, M. Saito, Y. Kanai, T. Watanabe, J. Nakamura and T. Uchijima, *Appl. Catal., A*, 1995, **125**, L199–L202.
17 G. L. Haller and D. E. Resasco, *Adv. Catal.*, 1989, **36**, 173–235.
18 J. Qu, X. W. Zhou, F. Xu, X. Q. Gong and S. C. E. Tsang, *J. Phys. Chem. C*, 2014, **118**, 24452–24466.
19 E. Gebauer-Henke, J. Grams, E. Szubiakiewicz, J. Farbotko, R. Touroude and J. Rynkowski, *J. Catal.*, 2007, **250**, 195–208.
20 Y. He, L. Liang, Y. Liu, J. Feng, C. Ma and D. Li, *J. Catal.*, 2014, **309**, 166–173.
21 A. N. Banerjee, N. Hamnabard and S. W. Joo, *Ceram. Int.*, 2016, **42**, 12010–12026.
22 C. C. Surdu-Bob, S. O. Saied and J. L. Sullivan, *Appl. Surf. Sci.*, 2011, **183**, 126–136.
23 C. Rameshan, W. Stadlmayr, S. Penner, H. Lorenz, L. Mayr, M. Havecker, R. Blume, T. Rocha, D. Teschner, A. Knop-Gericke, R. Schlogl, D. Zemlyanov, N. Memmel and B. Klotzer, *J. Catal.*, 2012, **290**, 126–137.
24 S. D. Wolter, B. P. Luther, D. L. Waltemyer, C. Onneby, S. E. Mohney and R. J. Molnar, *Appl. Phys. Lett.*, 1997, **70**, 2156–2158.
25 A. Haghofer, K. Föttinger, F. Girgsdies, D. Teschner, A. Knop-Gericke, R. Schlögl and G. Rupprechter, *J. Catal.*, 2012, **286**, 13–21.
26 S. E. Collins, J. J. Delgado, C. Mira, J. J. Calvino, S. Bernal, D. L. Chiavassa, M. A. Baltanás and A. L. Bonivardi, *J. Catal.*, 2012, **292**, 90–98.
27 O. Jacquet, X. Frogneux, C. Das Neves Gomes and T. Cantat, *Chem. Sci.*, 2013, **4**, 2127.
28 J. Liu, C. Guo, Z. Zhang, T. Jiang, H. Liu, J. Song, H. Fan and B. Han, *Chem. Commun.*, 2010, **46**, 5770–5772.
29 F. Solymosi, A. Erdöhelyi and M. Lancz, *J. Catal.*, 1985, **95**, 567–577.
30 H. Yoshida, S. Narisawa, S.-I. Fujita, R. Liu and M. Arai, *Phys. Chem. Chem. Phys.*, 2012, **14**, 4724–4733.
31 W. Huang, R. F. Lobo and J. G. Chen, *J. Mol. Catal. A: Chem.*, 2008, **283**, 158–165.
32 A. Vicente, G. Lafaye, C. Especel, P. Marecot and C. T. Williams, *J. Catal.*, 2011, **283**, 133–142.
33 A. Wille, P. Nickut and K. Al-Shamery, *J. Mol. Struct.*, 2004, **695–696**, 345–352.
34 J. H. T. Dellwig, J. Libuda, I. Meusel, G. Rupprechter, H. Unterhalt and H. J. Freund, *J. Mol. Catal. A: Chem.*, 2000, **162**, 51–66.

